XLI CILAMCE
XLI Ibero-Latin American Congress on Computational Methods in Engineering
16-19 November, 2020 FOZ DO IGUAÇU PARANÁ - BRAZIL

A von Mises stress-based topology optimization applying the standard finite-volume theory for continuum elastic structures

Marcelo Vitor Oliveira Araujo[1], Eduardo Nobre Lages[1], Márcio André Araújo Cavalcante[2]

[1]*Center of Technology, Federal University of Alagoas*
Av. Lourival Melo Mota, Tabuleiro do Martins, Maceió, 57072-900, Alagoas, Brazil
marcelo.vitor.o.a@gmail.com, enl@ctec.ufal.br
[2]*Campus of Engineering and Agricultural Sciences, Federal University of Alagoas*
BR-104, Rio Largo, 57100-000, Alagoas, Brazil
marcio.cavalcante@ceca.ufal.br

Abstract. Topology optimization algorithms want to establish the best material distribution inside of an analysis domain. In those optimization problems, usually there are some numerical problems to be overcome, such as the checkerboard pattern, mesh dependence, local minima, and occurrence of gray regions. This paper addresses a new topology optimization technique, where the objective is to minimize the equivalent average von Mises stress subject to a volume constraint and to apply the standard finite-volume theory for elastic stress analysis. The solid isotropic material with penalization (SIMP) approach is employed to avoid discrete optimization problems. The proposed optimization problem has shown efficiency, avoiding the occurrence of numerical instabilities, such as checkerboard pattern, mesh dependence, and local minima, when a sensitivity filter is employed. In the absence of filtering techniques, the proposed approach has shown efficiency by producing checkerboard-free optimized topologies with fewer bars, more robust bars, and well-defined "black and white" designs.

Keywords: topology optimization, finite-volume theory, equivalent von Mises stress minimization.

1 Introduction

Topology optimization seeks to establish the best material distribution inside an analysis domain and has been one of the main fields in structural analysis in the last decades. Since the pioneering work of Michell [1] and the reconstruction initiated by Bendsøe and Kikuchi [2], topology optimization has frequently been used to define the stiffest structure by minimizing the structural compliance. However, this is not the objective of most high-performance structural problems. A more realistic option would be to optimize the stress distribution inside the analysis domain by minimizing the equivalent von Mises stress subject to a volume constraint.

In a topology optimization problem, the interest is in defining which points of the analysis domain should be material or void, generating a "black and white" design. Therefore, the structural material distribution is obtained by a binary "0-1", where 0 indicates void and 1 indicates the presence of material. This kind of topology optimization leads to an integer programming problem, which has been shown an unfeasible approach. However, the material distribution can be also defined in terms of a continuum function, which defines the material relative density and can assume any real value between approximately 0, indicating void, and 1, indicating solid. In this case, the intermediate values of relative density must be avoided by penalization techniques.

An alternative technique to solve this problem is the solid isotropic material with penalization (SIMP) approach, which penalizes the intermediate values of relative densities to obtain a "black and white" project. In this method, the material properties are modeled by the element relative density raised to a certain power, which is recommended to be higher than 3, Bendsøe and Sigmund [3]. Although high penalty factors help to produce a well-defined "black and white" design, when the penalty factor is higher than one, in the SIMP approach, the optimization problem becomes nonconvex and there is no guarantee of a unique solution, Christensen and Klarbring [4].

Since the pioneering work of Bendsøe and Kikuchi [2] in the homogenization method of topology optimization, the finite element-based strategy for structural analysis has received wide attention and experienced

considerable progress, Wang and Wang [5]. An alternative technique to this method is the finite-volume theory, which employs the volume-average of the kinematic and static fields and imposes the boundary and continuity conditions in an averaged-sense. In addition, the satisfaction of differential equilibrium equations at the subvolume level, concomitant to kinematic and static continuity conditions established in a surface-averaged sense between common faces of adjacent subvolumes, are features that distinguish the finite-volume theory from the finite element method.

This contribution addresses a new approach for topology optimization based on the standard finite-volume theory, where the objective function is defined as the minimization of the structural equivalent von Mises stress. Comparison results between the minimization of equivalent von Mises stress and similar approaches based on the compliance minimization problem are provided, which demonstrate the efficiency of the proposed topology optimization technique.

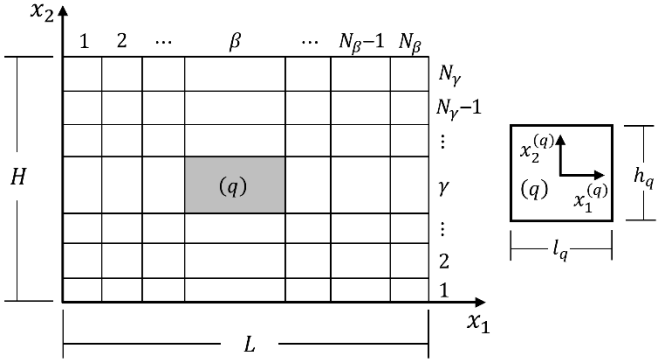

Figure 1. Discretized analysis domain and global coordinate system (left) and subvolume and local coordinate system (right)

2 Finite-volume theory

Figure 1 presents the adopted rectangular domain in $x_1 - x_2$ plane with $0 \leq x_1 \leq L$ and $0 \leq x_2 \leq H$, which is discretized in N_β horizontal subvolumes and N_γ vertical subvolumes. The subvolume dimensions are l_q and h_q for $q = 1, \dots, N_q$, where $N_q = N_\beta \cdot N_\gamma$ is the total number of subvolumes. Following Cavalcante and Pindera [6], the displacement of a subvolume q can be approximated by an incomplete quadratic version of Legendre polynomial expansion in the local coordinate system as follows:

$$u_i^{(q)} = W_{i(00)}^{(q)} + x_1^{(q)} W_{i(10)}^{(q)} + x_2^{(q)} W_{i(01)}^{(q)} + \frac{1}{2}\left(3\left(x_1^{(q)}\right)^2 - \frac{l_q^2}{4}\right) W_{i(20)}^{(q)} + \frac{1}{2}\left(3\left(x_2^{(q)}\right)^2 - \frac{h_q^2}{4}\right) W_{i(02)}^{(q)}, \tag{1}$$

where $i = 1{,}2$ and $W_{i(mn)}^{(q)}$ are unknown coefficients of the displacement field.

2.1 Local stiffness matrix

Following Bansal and Pindera [7], the surface-averaged displacement components of a generic subvolume can be defined as

$$\begin{aligned} \bar{u}_i^{(1,3)} &= \frac{1}{l_q} \int_{-\frac{l_q}{2}}^{\frac{l_q}{2}} u_i\left(x_1^{(q)}, \mp\frac{h_q}{2}\right) dx_1^{(q)} \\ \bar{u}_i^{(2,4)} &= \frac{1}{h_q} \int_{-\frac{h_q}{2}}^{\frac{h_q}{2}} u_i\left(\pm\frac{l_q}{2}, x_2^{(q)}\right) dx_2^{(q)} \end{aligned}, \tag{2}$$

where the superscript indicates the subvolume face number, indexed as illustrated in Fig. 2(a).

Substituting eq. (1) into eq. (2), eight expressions are obtained for the surface-averaged displacements, which can be organized as follows:

$$\bar{\boldsymbol{u}}^{(q)} = \boldsymbol{A}_{(8\times8)}^{(q)} \boldsymbol{W}^{(q)} + \boldsymbol{a}_{(8\times2)}^{(q)} \boldsymbol{W}_{(00)}^{(q)}, \tag{3}$$

where $\bar{\boldsymbol{u}}^{(q)}$ is the local surface-averaged displacement vector, $\boldsymbol{W}^{(q)}$ is the vector containing the first and second order unknown coefficients and $\boldsymbol{W}_{(00)}^{(q)}$ is the vector containing the zeroth order unknown coefficients. $\boldsymbol{A}_{(8\times8)}^{(q)}$ and

$\boldsymbol{a}_{(8\times2)}^{(q)}$ are matrixes that depend on the geometric features of the subvolume q.

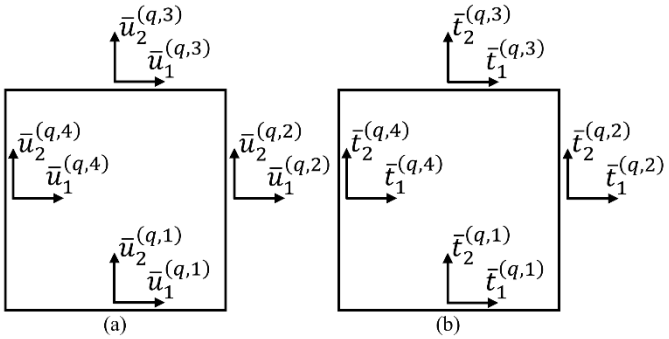

Figure 2. Surface-averaged quantities: (a) surface-averaged displacements and (b) surface-averaged tractions

Based on linear elastic stress analysis, the surface-averaged traction components can be evaluated as

$$\begin{aligned}\bar{t}_i^{(1,3)} &= \mp\frac{1}{l_q}\int_{-\frac{l_q}{2}}^{\frac{l_q}{2}}\sigma_{2i}\left(x_1^{(q)},\mp\frac{h_q}{2}\right)dx_1^{(q)}\\ \bar{t}_i^{(2,4)} &= \pm\frac{1}{h_q}\int_{-\frac{h_q}{2}}^{\frac{h_q}{2}}\sigma_{1i}\left(\pm\frac{l_q}{2},x_2^{(q)}\right)dx_2^{(q)}\end{aligned}. \tag{4}$$

Considering linear elastic isotropic materials, eight expressions for the surface-averaged tractions can be obtained in terms of the unknown coefficients

$$\bar{\boldsymbol{t}}^{(q)} = \boldsymbol{B}_{(8\times8)}^{(q)}\boldsymbol{W}^{(q)}, \tag{5}$$

where $\boldsymbol{B}_{(8\times8)}^{(q)}$ is the local surface-averaged traction vector, Fig. 2(b).

The local stiffness matrix can be established as

$$\boldsymbol{K}_{(8\times8)}^{(q)} = \boldsymbol{B}_{(8\times8)}^{(q)}\bar{\boldsymbol{A}}_{(8\times8)}^{(q)}, \tag{6}$$

where $\bar{\boldsymbol{A}}_{(8\times8)}^{(q)} = \left(\boldsymbol{A}_{(8\times8)}^{(q)}\right)^{-1} - \left(\boldsymbol{A}_{(8\times8)}^{(q)}\right)^{-1}\boldsymbol{a}_{(8\times2)}^{(q)}\bar{\boldsymbol{a}}_{(2\times8)}^{(q)}$ and $\bar{\boldsymbol{a}}_{(2\times8)}^{(q)} = \left[\left(\sum_{p=1}^{4}\boldsymbol{B}_{(2\times8)}^{(q,p)}L_p^{(q)}\right)\left(\boldsymbol{A}_{(8\times8)}^{(q)}\right)^{-1}\boldsymbol{a}_{(8\times2)}^{(q)}\right]^{-1}\left(\sum_{p=1}^{4}\boldsymbol{B}_{(2\times8)}^{(q,p)}L_p^{(q)}\right)\left(\boldsymbol{A}_{(8\times8)}^{(q)}\right)^{-1}$. In this case, $L_1^{(q)} = l_q$, $L_2^{(q)} = h_q$, $L_3^{(q)} = l_q$ and $L_4^{(q)} = h_q$ are the faces' lengths of a generic subvolume q.

3 Topology optimization problem

3.1 Compliance minimization problem

The total strain energy of a structure can be defined as

$$U = \iiint_\Omega \frac{1}{2}\boldsymbol{\sigma}^T\boldsymbol{\varepsilon}\,d\Omega = \iiint_\Omega \frac{1}{2}\boldsymbol{\varepsilon}^T\boldsymbol{C}\boldsymbol{\varepsilon}\,d\Omega, \tag{7}$$

where $\boldsymbol{\sigma}$ is the stress tensor, $\boldsymbol{\varepsilon}$ is the strain tensor and $\boldsymbol{C}$ is the stiffness tensor. Considering the assumptions of the elasticity theory and the displacement field approximation presented in eq. (1), the local strain tensor is given as

$$\boldsymbol{\varepsilon}^{(q)} = \boldsymbol{E}^{(q)}\left(x_1^{(q)},x_2^{(q)}\right)\boldsymbol{W}^{(q)}, \tag{8}$$

where $\boldsymbol{E}^{(q)}\left(x_1^{(q)},x_2^{(q)}\right)$ is the kinematic matrix that relates the strain tensor components with the unknown coefficients.

Therefore, the specific strain energy can be evaluated as

$$U^{(q)} = \int_{-\frac{h_q}{2}}^{\frac{h_q}{2}}\int_{-\frac{l_q}{2}}^{\frac{l_q}{2}}\frac{1}{2}\boldsymbol{\varepsilon}^T\boldsymbol{C}\boldsymbol{\varepsilon}\,dx_1^{(q)}\,dx_2^{(q)} = \frac{1}{2}\boldsymbol{W}^{(q)}\boldsymbol{D}^{(q)}\boldsymbol{W}^{(q)}, \tag{9}$$

where $\boldsymbol{D}^{(q)} = \int_{-\frac{h_q}{2}}^{\frac{h_q}{2}} \int_{-\frac{l_q}{2}}^{\frac{l_q}{2}} \frac{1}{2} \left(\boldsymbol{E}^{(q)}\right)^T \boldsymbol{C}^{(q)} \boldsymbol{E}^{(q)} \, dx_1^{(q)} \, dx_2^{(q)}$. The total strain energy is obtained considering the individual contribution of each subvolume by

$$U = \iiint_{\Omega} \bar{U} \, d\Omega = \sum_{q=1}^{N_q} U^{(q)}. \tag{10}$$

The topology optimization problem based on the power-law approach for compliance minimization can be written as

$$\begin{cases} \min c(\boldsymbol{\rho}) = \sum_{q=1}^{N_q} \left(\rho_q\right)^p \boldsymbol{W}^{(q)} \boldsymbol{D}^{(q)} \boldsymbol{W}^{(q)} \\ \text{subject to:} \\ \frac{V(\boldsymbol{\rho})}{\bar{V}} = f \\ 0 < \rho_{min} \leq \rho_q \leq 1 \end{cases}, \tag{11}$$

where $V(\boldsymbol{\rho})$ and $\bar{V}$ are the material and reference domain volumes, respectively, $\boldsymbol{\rho}$ is the relative density tensor, p is the penalty factor, f is the prescribed volume fraction and ρ_{min} is the minimum relative density to avoid singularity in the stiffness matrix. This optimization problem is solved using the optimality criteria (OC) method and the damping factor is adjusted to avoid the oscillatory phenomenon, which is caused by the low-density regions in the optimized structure.

3.2 Average von Mises stress minimization problem

The average equivalent von Mises stress of a structure can be evaluated by

$$\bar{\sigma}_v(\boldsymbol{\rho}) = \frac{1}{\bar{V}} \iiint_{\Omega} \sigma_v(\boldsymbol{x}, \boldsymbol{\rho}) \, d\Omega = \frac{1}{\bar{V}} \sum_{q=1}^{N_q} \iiint_{\mathrm{V}_q} \sigma_v^{(q)}\left(\boldsymbol{x}^{(q)}, \rho_q\right) d\mathrm{V}_q = \sum_{q=1}^{N_q} f_q \bar{\sigma}_v^{(q)}\left(\rho_q\right), \tag{12}$$

where $\sigma_v^{(q)}$ and V_q are the von Mises stress and volume of a subvolume q, respectively, f_q is the subvolume volume fraction and $\bar{\sigma}_v^{(q)}\left(\rho_q\right)$ is the average von Mises stress in the subvolume q, which is given by

$$\bar{\sigma}_v^{(q)}\left(\rho_q\right) = \frac{1}{V_q} \iiint_{\mathrm{V}_q} \sigma_v^{(q)}\left(\boldsymbol{x}^{(q)}, \rho_q\right) d\mathrm{V}_q = \frac{1}{V_q} \int_{-\frac{h_q}{2}}^{\frac{h_q}{2}} \int_{-\frac{l_q}{2}}^{\frac{l_q}{2}} \sigma_v^{(q)}\left(x_1^{(q)}, x_2^{(q)}, \rho_q\right) dx_1^{(q)} \, dx_2^{(q)}. \tag{13}$$

Considering the plane stress state, the von Mises stress of the subvolume q is given by

$$\left(\sigma_v^{(q)}\left(\boldsymbol{x}^{(q)}, \rho_q\right)\right)^2 = \left(\boldsymbol{\sigma}^{(q)}\left(\boldsymbol{x}^{(q)}, \rho_q\right)\right)^T \boldsymbol{P} \boldsymbol{\sigma}^{(q)}\left(\boldsymbol{x}^{(q)}, \rho_q\right), \tag{14}$$

where $\boldsymbol{\sigma}^{(q)}\left(\boldsymbol{x}^{(q)}, \rho_q\right) = \left[\sigma_{11}^{(q)}\left(\boldsymbol{x}^{(q)}, \rho_q\right) \quad \sigma_{22}^{(q)}\left(\boldsymbol{x}^{(q)}, \rho_q\right) \quad \sigma_{12}^{(q)}\left(\boldsymbol{x}^{(q)}, \rho_q\right)\right]^T = \boldsymbol{C}^{(q)}\left(\rho_q\right) \boldsymbol{\varepsilon}^{(q)}$ is the local stress tensor and

$$\boldsymbol{P} = \begin{bmatrix} 1 & -1/2 & 0 \\ -1/2 & 1 & 0 \\ 0 & 0 & 3 \end{bmatrix}. \tag{15}$$

Thus, the local von Mises stress can be obtained by

$$\sigma_v^{(q)}\left(\boldsymbol{x}^{(q)}, \rho_q\right) = \left(\rho_q\right)^p \left[\left(\bar{\boldsymbol{u}}^{(q)}\right)^T \left(\bar{\boldsymbol{A}}_{(8\times8)}^{(q)}\right)^T \left(\boldsymbol{E}^{(q)}\left(\boldsymbol{x}^{(q)}\right)\right)^T \left(\boldsymbol{C}^{(q)}(1)\right)^T \boldsymbol{P} \boldsymbol{C}^{(q)}(1) \boldsymbol{E}^{(q)}\left(\boldsymbol{x}^{(q)}\right) \bar{\boldsymbol{A}}_{(8\times8)}^{(q)} \bar{\boldsymbol{u}}^{(q)}\right]^{\frac{1}{2}}, \tag{16}$$

where $\boldsymbol{C}^{(q)}(1)$ is the stiffness tensor correspondent to a unitary relative density. Finally, the proposed topology optimization problem can be written as

$$\begin{cases} \min \bar{\sigma}_v(\boldsymbol{\rho}) = \sum_{q=1}^{N_q} f_q \bar{\sigma}_v^{(q)}\left(\rho_q\right) \\ \text{subject to:} \\ \frac{V(\boldsymbol{\rho})}{\bar{V}} = \sum_{q=1}^{N_q} \rho_q f_q \\ 0 < \rho_{min} \leq \rho_q \leq 1 \end{cases}. \tag{17}$$

In this case, the double integration presented in eq. (13) can be solved by employing the Simpsons' rule for 3×3 integration points. Therefore, the optimization presented in eq. (17) can be solved using the OC method, where the objective function gradient is given by

$$\frac{\partial \bar{\sigma}_v}{\partial \rho_q} = -\frac{1}{\bar{V}} p(\rho_q)^{p-1} \int_{-\frac{h_q}{2}}^{\frac{h_q}{2}} \int_{-\frac{l_q}{2}}^{\frac{l_q}{2}} \sigma_v^{(q)} \left(x_1^{(q)}, x_2^{(q)}, 1\right) dx_1^{(q)} dx_2^{(q)}. \tag{18}$$

3.3 Mesh-independency filter

Following Sigmund [8], to avoid the occurrence of mesh dependence, it is suggested to modify the subvolume sensitivities in some approaches using the following expression:

$$\frac{\partial \bar{\sigma}_v}{\partial \rho_q} \text{or} \frac{\partial c}{\partial \rho_q} = \frac{1}{\rho_q \sum_{e=1}^{N_q} \hat{H}_e} \sum_{e=1}^{N_q} \hat{H}_e \rho_e \left(\frac{\partial c}{\partial \rho_e} \text{or} \frac{\partial \bar{\sigma}_v}{\partial \rho_q}\right), \tag{19}$$

where $\hat{H}_e$ is the convolution operator (weighting function) given as

$$\hat{H}_e = R - \text{dist}(q,e) \text{ for } \text{dist}(q,e) \leq R \text{ and } \hat{H}_e = 0 \text{ otherwise}, \tag{20}$$

where $\text{dist}(q,e)$ is the distance between the subvolume center of q and e. To consider only the contributions of neighbor subvolumes (with shared nodes), it is adopted a filter radius of $R = 1.01\sqrt{l_q^2 + h_q^2}$.

4 Results and discussion

The cantilever beam, shown in Fig. 3, is a classical problem in topology optimization. Here, this example is employed for efficiency comparison between different topology optimization approaches based on the standard finite-volume. For the different topology optimization approaches, it is used the continued penalization scheme, where the penalty factor increases gradually ($\Delta p = 0.5$) from 1 to 4, as suggested by Talischi et al. [9]. As a criterion of convergence, the maximum tolerance for the change in design variables is set up as 1%.

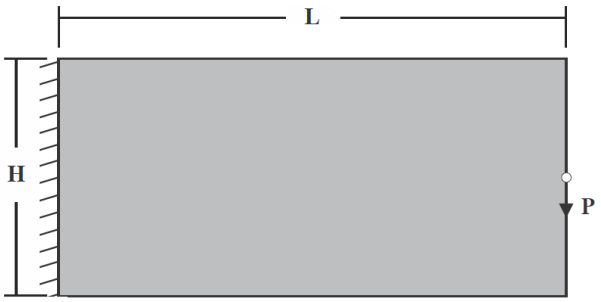

Figure 3. Cantilever beam

The damping factor is adjusted, for the compliance minimization problem without filtering, to avoid the oscillatory phenomenon during the optimization process. The proposed optimization problem consists of minimizing the structural compliance or the average von Mises stress subject to a volume constraint of 40% of the total volume. The computational environment, in terms of programming language and machine, can be described as MatLab R2018a/Intel® Core™ i7-8550U CPU @ 1.80 GHz 1.99 GHz/16.0 GB RAM/64-bits.

Figure 4 shows the optimized topologies for each topology optimization approach, considering the absence of filtering technique. The approach based on the compliance minimization problem has presented the same local minima and mesh dependence issues presented in Araujo et al. [10]. In this case, the damping factor is adjusted to $1/2.6$ to avoid divergence during the optimization process, as suggested by Araujo et al. [10]. For the average stress minimization approach, the damping factor is set up as $1/2$, providing a fast convergence to the optimization problem. Similarly, the topology optimization problem based on the averaged stress minimization has presented some numerical instabilities, such as mesh dependence and local minima, however, the obtained "black and white" designs are free of intermediate values of relative density, and present fewer bars and thicker bars. Additionally, Fig. 5 presents the von Mises stress distributions for the optimized topologies. As expected, the topology optimization technique based on the averaged von Mises stress minimization has reduced the stress concentration along the slender bars, especially for the finest mesh.

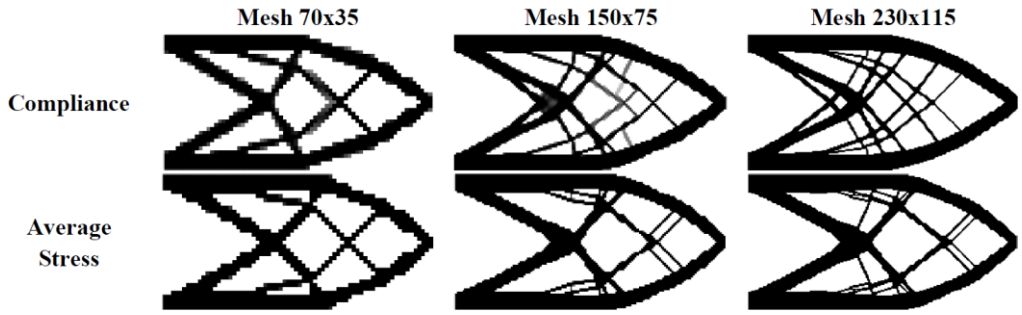

Figure 4. Optimized topologies without filtering technique

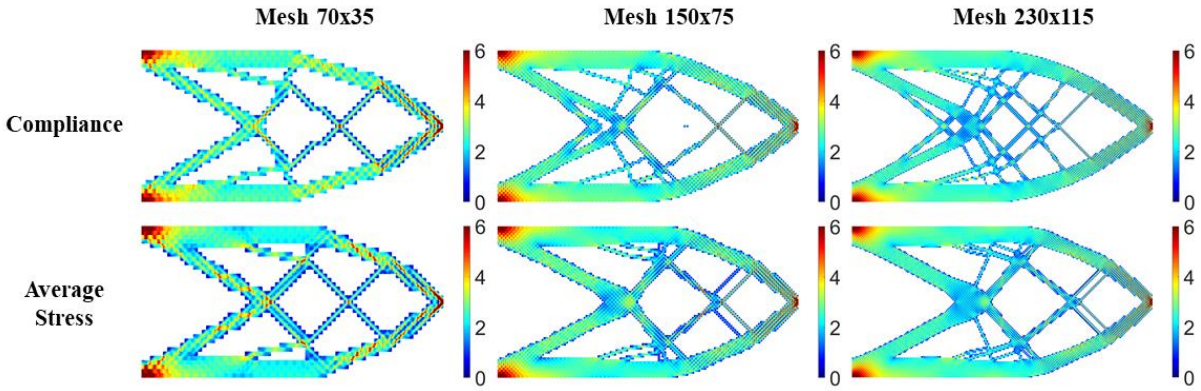

Figure 5. Von Mises stress distributions (MPa) of the optimized topologies obtained without filtering technique

Similarly, Fig. 6 presents the optimized topologies obtained for the proposed approaches employing the sensitivity filter. In the scenario of filtering technique, the adopted damping factor is $1/2$, as recommended for faster convergence, Araujo et al. [10]. In fact, the topology optimization problem based on the average stress minimization has presented less mesh sensitivity. In addition, this approach has provided optimized topologies with fewer and more robust bars, which controls better some numerical issues such as mesh dependence and local minima. Although the topology optimization problem for compliance minimization, considering filtering, has presented more slender bars, the optimized topology obtained by this approach has shown the same force-displacement curve of the topology obtained employing the average stress minimization problem, for the finest mesh, as shown in Fig. 8. At the same time, Fig. 7 shows the von Mises stress distributions obtained for the optimized topologies presented in Fig. 6, providing less stress concentration when the average stress minimization problem is employed for the finest mesh.

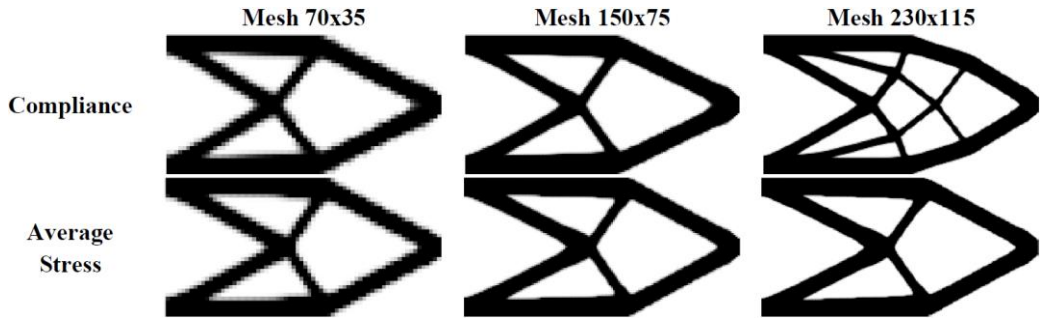

Figure 6. Optimized topologies with filtering technique

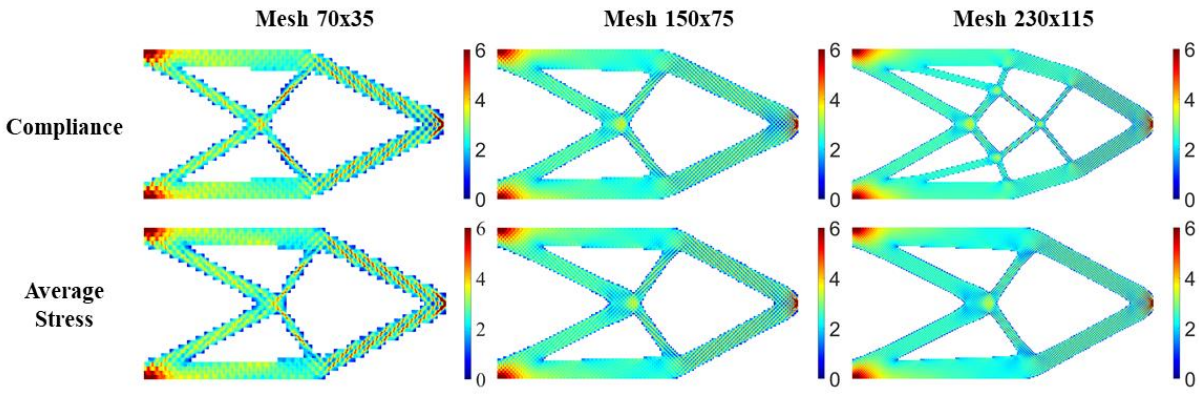

Figure 7. Von Mises stress distributions (MPa) of the optimized topologies employing the filtering technique

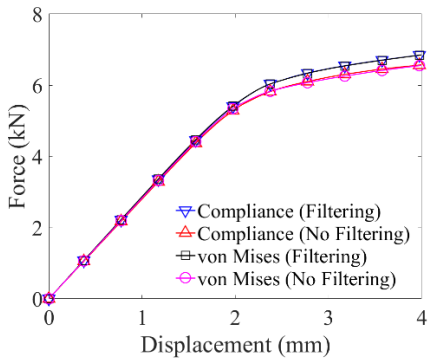

Figure 8. Force-displacement diagram

Table 1 presents the investigated numerical aspects, such as the number of iterations, computational cost, von Mises average stress, and compliance. In fact, the approach employing the average von Mises minimization with filtering has presented the fastest convergence by reducing the total number of iterations, while the approach based on the compliance minimization problem, in the absence of filtering technique, has presented the highest computational cost and total number of iterations, for the finest mesh. Although the average von Mises stress for the stress-based topology optimization, considering filtering, has been higher than the approach based on the compliance minimization problem, this approach has optimized the structural compliance, for the finest mesh.

Table 1. Convergence analysis

Analysis	Mesh	Number of Iterations	Processing Time	Average von Mises stress (MPa)	Compliance (MJ)
Compliance (No filtering)	70 × 35	156	29 min 21s	2.457	4.685
	150 × 75	329	6 h 2 min 40 s	2.428	4.484
	230 × 115	630	54 h 5 min 35 s	2.417	4.335
von Mises (No filtering)	70 × 35	198	1 min 3 s	2.464	5.547
	150 × 75	424	3 h 8 min 19 s	2.446	5.358
	230 × 115	450	21 h 26 min 51 s	2.435	5.348
Compliance (Filtering)	70 × 35	327	35 min 52 s	2.462	4.903
	150 × 75	523	7 h 2 min 36 s	2.447	4.441
	230 × 115	569	44 h 9 min 25 s	2.427	4.375
von Mises (Filtering)	70 × 35	125	4 min 41 s	2.472	4.928
	150 × 75	216	1 h 52 min	2.445	4.458
	230 × 115	399	18 h 25 min 17 s	2.437	4.352

5 Conclusions

The new topology optimization for the average equivalent von Mises stress minimization problem based on the standard finite-volume theory has shown to be efficient, especially when a sensitivity filter is employed. This technique could produce efficient optimized topologies, where the mesh dependence and local minima issues are better controlled when compared to the compliance minimization problem. In addition, this technique could reduce the total required number of iterations, providing the fastest convergence for the analyzed approaches.

In the absence of filtering techniques, the average von Mises stress minimization problem has obtained optimized topologies with fewer bars and more robust bars, where the "black and white" designs are composed of approximately 0 or 1 densities, which is a desired feature in topology optimization problems. Based on the presented results, the continuation of this investigation is justified by exploring the most different aspects of the finite-volume theory and analyzing other examples.

Acknowledgements. The authors acknowledge the financial support provided by CAPES and CNPq.

Authorship statement. The authors hereby confirm that they are the sole liable persons responsible for the authorship of this work, and that all material that has been herein included as part of the present paper is either the property (and authorship) of the authors, or has the permission of the owners to be included here.

References

[1] A. G. M. Michell. "The limits of economy of material in frame structures". *The London, Edinburgh, and Dublin Philosophical Magazine and Journal of Science*, vol. 8, n. 47, pp. 589–597, 1904.
[2] M. P. Bendsøe and N. Kikuchi. "Generating optimal topologies in structural design using a homogenization method". *Computer Methods in Applied Mechanics and Engineering*, vol. 71, n. 2, pp. 197–224, 1988.
[3] M. P. Bendsøe and O. Sigmund. "Material interpolation schemes in topology optimization". *Archive of Applied Mechanics*, vol. 69, n. 9-10, pp. 635–654, 1999.
[4] P. W. Christensen and A. Klarbring. An introduction to structural optimization. Linköping: Springer Science & Business Media, 2009.
[5] S. Wang and M. Y. Wang. "Radial basis function and level set method for structural topology optimization". International Journal for Numerical Methods in Engineering, vol. 65, n. 12, pp. 2060–2090, 2006.
[6] M. A. A. Cavalcante and M.-J. Pindera. "Generalized finite-volume theory for elastic stress analysis in solid mechanics – part I: framework". *Journal of Applied Mechanics*, vol. 79, n. 5, pp. 051006, 2012.
[7] Y. Bansal and M.-J. Pindera. "Efficient reformulation of the thermoelastic higher-order theory for functionally graded materials". *Journal of Thermal Stress*, vol. 26, n. 11-12, pp. 1055–1092, 2003.
[8] O. Sigmund. "A 99-line topology optimization code written in Matlab". *Structural and Multidisciplinary Optimization*, vol. 21, n. 2, pp. 120–127, 2001.
[9] C. Talischi, G. H. Paulino, A. Pereira, I. F. M. Menezes. "PolyTop: a Matlab implementation of a general topology optimization framework using unstructured polygonal finite element meshes". Structural and Multidisciplinary Optimization, vol. 45, n. 3, pp. 329–357, 2012.
[10] M. V. O. Araujo, E. N. Lages, M. A. A. Cavalcante. "Checkerboard free topology optimization for compliance minimization applying the finite-volume theory". *Mechanics Research Communications*, vol. 108, pp. 103581, 2020.